

---

# Self-hardening calcium phosphate cement–mesh composite: Reinforcement, macropores, and cell response

---

Hockin H. K. Xu,<sup>1</sup> Carl G. Simon, Jr.<sup>2</sup>

<sup>1</sup>Paffenbarger Research Center, American Dental Association Foundation, National Institute of Standards and Technology, Gaithersburg, Maryland 20899

<sup>2</sup>Polymers Division, National Institute of Standards and Technology, Gaithersburg, Maryland 20899

Received 13 November 2002; revised 5 November 2003; accepted 12 November 2003

Published online 17 February 2004 in Wiley InterScience (www.interscience.wiley.com). DOI: 10.1002/jbm.a.20124

**Abstract:** Calcium phosphate cement (CPC) self-hardens to form hydroxyapatite, has excellent osteoconductivity and bone-replacement ability, and is promising for craniofacial and orthopedic repair. However, its low strength limits CPC to only nonstress repairs. This study aimed to reinforce CPC with meshes to increase strength, and to form macropores in CPC for bone ingrowth after mesh dissolution. A related aim was to evaluate the biocompatibility of the new CPC–mesh composite. Absorbable polyglactin meshes, a copolymer of poly(glycolic) and poly(lactic) acids, were incorporated into CPC to provide strength and then form interconnected cylindrical macropores suitable for vascular ingrowth. The composite flexural strength, work-of-fracture, and elastic modulus were measured as a function of the number of mesh sheets in CPC ranging from 1 (a mesh on the tensile side of the specimen) up to 13 (mesh sheets throughout the entire specimen), and as a function of immersion time in a physiological solution from 1 to 84 days. Cell culture was performed with osteoblast-like cells and the cell viability was quantified using an enzymatic assay. The strengths (mean  $\pm$  SD;  $n = 6$ ) of CPC containing 13 or 6 meshes were  $24.5 \pm 7.8$  and  $19.7 \pm 4.3$  MPa, respectively,

not significantly different from each other; both were significantly higher than  $8.8 \pm 1.9$  MPa of CPC without mesh (Tukey's at 0.95). The work-of-fracture of CPC with 13 or 6 meshes was  $3.35 \pm 0.80$  and  $2.95 \pm 0.58$  kJ/m<sup>2</sup>, respectively, two orders of magnitude higher than  $0.021 \pm 0.006$  kJ/m<sup>2</sup> of CPC without mesh. Interconnected macropores were formed in CPC at 84 days' immersion. The new CPC–mesh formulation supported the adhesion, spreading, proliferation, and viability of osteoblast-like cells *in vitro*. In conclusion, absorbable meshes in CPC increased the implant strength by three-fold and work-of-fracture by 150 times; interconnected macropores suitable for bone ingrowth were created in CPC after mesh dissolution. The higher strength may help extend the use of CPC to larger stress-bearing repairs, and the macropores may facilitate tissue ingrowth and integration of CPC with adjacent bone. © 2004 Wiley Periodicals, Inc. *J Biomed Mater Res* 69A: 267–278, 2004

**Key words:** calcium phosphate cement; hydroxyapatite; mesh reinforcement; macroporous scaffold; cell culture; biocompatibility

---

## INTRODUCTION

There is an increasing need for dental, craniofacial, and orthopedic biomaterials as the world population

Certain commercial materials and equipment are identified in this article to specify experimental procedures. In no instance does such identification imply recommendation by the National Institute of Standards and Technology or the American Dental Association Health Foundation or that the material identified is necessarily the best available for the purpose.

Correspondence to: H. H. K. Xu; e-mail: hockin.xu@nist.gov

Contract grant sponsor: National Institute of Dental and Craniofacial Research; contract grant numbers: DE12476 and DE14190

Contract grant sponsor: National Institute of Standards and Technology

Contract grant sponsor: American Dental Association Foundation

ages.<sup>1,2</sup> Hydroxyapatite has been useful because of its chemical and crystallographic similarity to the carbonated apatite in human teeth and bones.<sup>1,2</sup> Several calcium phosphate cements (CPCs) self-harden to form hydroxyapatite and possess excellent osteoconductivity and biocompatibility.<sup>3–6</sup> One CPC<sup>3</sup> is composed of a mixture of fine particles of tetracalcium phosphate [TTCP: Ca<sub>4</sub>(PO<sub>4</sub>)<sub>2</sub>O] and dicalcium phosphate anhydrous (DCPA: CaHPO<sub>4</sub>).<sup>7,8</sup> The CPC powder can be mixed with water to form a thick paste that can be sculpted during surgery to conform to the defects in hard tissues; the paste then sets *in situ* to form hydroxyapatite.<sup>7–12</sup> CPC is highly promising for use in a wide range of applications,<sup>3,7,8</sup> including repair of periodontal bone defects and tooth defects, reconstruction of frontal sinus and augmentation of craniofacial skeletal defects,<sup>7–10</sup> and use in endodontics.<sup>11,12</sup> However, the relatively low strength and susceptibility to brittle fracture of CPC have limited its use to only non-load-bearing applications.<sup>8–10</sup> For orthope-

dic repair, the use of CPC was limited to the reconstruction of non-stress-bearing bone.<sup>10</sup> In periodontal repair, tooth mobility resulted in the early fracture and eventual exfoliation of the brittle CPC implants.<sup>13</sup>

Fibers have been incorporated into poly(methyl methacrylate) bone cements and other biomaterials to enhance the fracture resistance.<sup>14–16</sup> In a recent study, an absorbable mesh was placed on the tensile side of a CPC specimen, resulting in significantly increased work-to-fracture<sup>17</sup>; however, the strength and elastic modulus were not reported, and the thin mesh was limited to one surface of the specimen with no meshes throughout the thickness of the specimen.<sup>17</sup> In addition, no macropores were produced in CPC for bone ingrowth in that study.<sup>17</sup> In other studies, fibers of various lengths and volume fractions were randomly mixed into CPC resulting in substantial increases in the strength and work-of-fracture (toughness) of the composites.<sup>18,19</sup>

Macropores have been built into implants to facilitate vascular ingrowth.<sup>20–23</sup> One study incorporated water-soluble mannitol crystals in CPC, which were then extracted by soaking in water producing macropores in the shapes of the entrapped crystals.<sup>24</sup> However, although CPC without macropores was not recommended for stress-bearing restorations,<sup>8–10</sup> the macropores rendered CPC even weaker mechanically.<sup>24</sup> Therefore, in our recent study,<sup>25</sup> aramid fibers were used to develop strong and macroporous CPC. Whereas the implant strength was substantially increased, the fibers were stable and not bioresorbable. In a further study, we incorporated resorbable fibers into CPC to obtain reinforcement and then macroporosity after fiber dissolution.<sup>26</sup> In both studies, the fibers were randomly mixed into the bulk CPC.

In the present study, absorbable mesh sheets made of interconnected fiber bundles were incorporated into CPC to be suitable for skull or shell-structure repairs, and to achieve short-term strength and then interconnected macropores for tissue ingrowth. The flexural strength, elastic modulus, and work-of-fracture (toughness) of the specimens were measured versus number of mesh sheets in CPC and immersion time in a physiological solution. The mesh reinforcement mechanisms and macropore formation were examined with scanning electron microscopy (SEM). Because cell culture toxicity assays are the international standard for the initial screening of materials for biocompatibility,<sup>27</sup> we performed *in vitro* cell culture to evaluate the biocompatibility of the new cement formulation.

## MATERIALS AND METHODS

### Specimens for the effect of number of meshes on mechanical properties

The CPC specimens were made by mixing the CPC powder with distilled water to form a paste, which was then

placed into a mold and allowed to convert to microcrystalline hydroxyapatite. The CPC powder consisted of a mixture of TTCP and DCPA<sup>3</sup> with a TTCP/DCPA mole ratio of 1 (BoneSource; Osteogenics, Winston-Salem, NC). The TTCP powder had a mean particle size of approximately 17  $\mu\text{m}$ , and the DCPA powder had a mean particle size of approximately 1  $\mu\text{m}$ .

An absorbable fiber mesh (Vicryl, polyglactin 910; Ethicon, Somerville, NJ), a copolymer of poly(glycolic) and poly(lactic) acids, was used because polyglactin 910 fibers are clinically used as sutures. In addition, polyglactin 910 fibers had a relatively high strength.<sup>18,26</sup> The mesh was cut with a pair of sharp scissors into sheets of approximately  $4 \times 25$  mm. The CPC powder was mixed with distilled water using a spatula at a powder/liquid mass ratio of 3:1 to form a paste as described in previous studies.<sup>26</sup> A prescribed number of mesh sheets were placed into a stainless steel mold of  $3 \times 4 \times 25$  mm. The paste was then placed with the spatula on top of the mesh and lightly pressed to fill the pores of the mesh and to fill the rest of the mold. To study the effect of the number of mesh sheets, the following numbers of sheets of mesh were incorporated into the prospective tensile side of the CPC specimens: 0 (CPC control without mesh), 1, 3, 6, and 13. Because the mesh thickness was approximately 230  $\mu\text{m}$ , 13 sheets of mesh just filled the entire mold with a height of 3 mm so that the specimen contained sheets of mesh throughout its entire thickness. The CPC paste filled the holes of the mesh and set to form a cohesive specimen. The composite in the mold was covered with two mechanically clamped glass slides. The assembly was incubated in a humidifier with 100% humidity at 37°C for 4 h. Six specimens were made at each mesh number. The hardened specimens were demolded, immersed in a saline solution (0.9% sodium chloride; Baxter Healthcare, Deerfield, IL), and stored in an oven at 37°C for 20 h before flexural testing.

### Specimens for the effect of immersion time on mechanical properties

To investigate the effect of immersion time on mesh dissolution and specimen properties, an intermediate number of six sheets of mesh was incorporated into the prospective tensile side of each specimen. After setting in the humidifier, the specimens were immersed, as described above, for each of six periods of time: 1, 14, 21, 28, 42, and 84 days. Six specimens were made for each immersion time period. CPC control specimens without mesh were also fabricated and immersed.

### Mechanical testing

A standard three-point flexural test<sup>28</sup> with a span of 20 mm was used to fracture the specimens at a crosshead speed of 1 mm/min on a computer-controlled Universal Testing Machine (model 5500R; Instron Corp., Canton, MA). The side of specimen with the mesh was placed in tension and the mesh plane was normal to the applied load. The following properties were evaluated: flexural strength, elastic

modulus, and work-of-fracture (the energy required to fracture the specimen obtained from the area under the load-displacement curve divided by the specimen's cross-section area).<sup>29</sup> The displacement was estimated from the crosshead travel. After the CPC matrix had cracked, the mesh-reinforced specimens were still intact because the meshes bridged the cracks and supported the applied load. The test was stopped at a maximum crosshead displacement of 2 mm for a consistent calculation of work-of-fracture. It would be ideal to report both the first cracking strength and the ultimate strength (calculated from the highest load on the load-displacement curve).<sup>29</sup> However, the self-hardened CPC-based specimens in the present study contained many intrinsic micropores<sup>25</sup> and the first cracking strength could not always be determined. Therefore, the ultimate strength was measured and reported as the flexural strength of the specimens.

### Specimens for cell culture

Cell culture specimens were made under aseptic conditions in disc-shaped molds with a diameter of 10 mm and a height of 4 mm using UV-sterilized CPC powder and sterile water. The same absorbable mesh was cut to disks of approximately 10 mm in diameter. As described above, six sheets of mesh were incorporated into the prospective cell seeding side of each specimen. The same CPC powder-to-liquid ratio was used and the specimens were hardened in a cell incubator (100% humidity and 37°C) for 24 h. Eighteen CPC–mesh disks and 18 CPC control discs were made and divided into three groups, with six discs of each material in each group. These three groups of specimens were used for 1-day cell culture, 14-day cell culture, and an enzymatic assay, respectively.

### Cell culture and fluorescence microscopy

Established protocols for the culture and passage of MC3T3-E1 cells were followed.<sup>30,31</sup> Cells were obtained from Riken Cell Bank (Hirosaka, Japan) and cultured in flasks (75-cm<sup>2</sup> surface area) at 37°C in a fully humidified atmosphere at 5% CO<sub>2</sub> (volume fraction) in  $\alpha$  modified Eagle's minimum essential medium (BioWhittaker, Inc., Walkersville, MD). The medium was supplemented with 10% (volume fraction) fetal bovine serum (Gibco, Rockville, MD) and kanamycin sulfate (Sigma, Inc., St. Louis, MO). The medium was changed twice weekly, and the cultures were passaged with 2.5 g/L trypsin (0.25% mass fraction) containing 1 mmol/L ethylenediaminetetraacetic acid (Gibco) once per week. Cultures of 90% confluent MC3T3-E1 cells were trypsinized, washed, and suspended in fresh media. CPC–mesh and CPC control specimens were placed one each into the wells of a 24-well plate (BD Biosciences, Bedford, MA). Fifty thousand cells diluted into 2 mL of media were added to wells containing the discs or to empty wells (tissue culture polystyrene controls, or "TCPS control") and incubated for 1 or 14 days (2 mL of fresh media every 2 days).<sup>30</sup>

After 1 or 14 days, the media was removed and the cells were washed with 1 mL of fresh media. Cells were then stained for 10 min in media containing 2  $\mu$ mol/L calcein-AM and 2  $\mu$ mol/L ethidium homodimer-1 (Molecular Probes, Eugene, OR) and viewed by epifluorescence microscopy for six CPC–mesh specimens, six CPC control specimens, and six TCPS control wells.

### Wst-1 cell viability assay

Cells grown on CPC–mesh or CPC control for 14 days were analyzed for viability using the Wst-1 assay which measures mitochondrial dehydrogenase activity.<sup>32</sup> Wst-1 refers to 2-(4-iodophenyl)-3-(4-nitrophenyl)-5-(2,4-disulfophenyl)-2H-tetrazolium, monosodium salt (Dojindo, Gaithersburg, MD). Specimens with cells were transferred to clean wells in a 24-well plate and rinsed with 1 mL of Tyrode's Hepes buffer (140 mmol/L NaCl, 0.34 mmol/L Na<sub>2</sub>HPO<sub>4</sub>, 2.9 mmol/L KCl, 10 mmol/L Hepes, 12 mmol/L NaHCO<sub>3</sub>, 5 mmol/L glucose, pH 7.4). One milliliter of Tyrode's Hepes buffer and 0.1 mL of Wst-1 solution (5 mmol/L Wst-1 and 0.2 mmol/L 1-methoxy-5-methylphenazinium methylsulfate in water) were added to each well and incubated at 37°C for 2 h. Blank wells were also prepared that contained only buffer and Wst-1 solution. After 2 h, 0.2 mL of each reaction mixture was transferred to a 96-well plate and the absorbance at 450 nm was measured with a microplate reader (Wallac 1420 Victor<sup>2</sup>; PerkinElmer Life Sciences, Gaithersburg, MD). The assay was performed with six CPC–mesh specimens, six CPC control specimens, and six blank wells. The absorbance for the blank wells was subtracted from the data.

A scanning electron microscope (model JSM-5300; JEOL, Peabody, MA) was used to examine gold-sputtered specimens for mesh reinforcement mechanisms, macropore formation, and cells. Cells cultured for 1 day on specimens were rinsed with saline, fixed with 1% glutaraldehyde, subjected to graded alcohol dehydrations, rinsed with hexamethyldisilazane, and then sputter coated with gold. One standard deviation was given in this article for comparative purposes as the estimated standard uncertainty of the measurements. These values should not be compared with data obtained in other laboratories under different conditions. One-way analysis of variance was performed to detect significant differences in data. Tukey's multiple comparison procedures were used to compare the data at a family confidence coefficient of 0.95.

## RESULTS

Figure 1(A) shows a SEM micrograph of the absorbable mesh. The mesh had bundles and nodes with diameters of 100–200  $\mu$ m, which after dissolution would create interconnected cylindrical macropores in CPC suitable for vascular ingrowth. These meshes provided substantial reinforcement to CPC before mesh dissolution. The CPC control without mesh

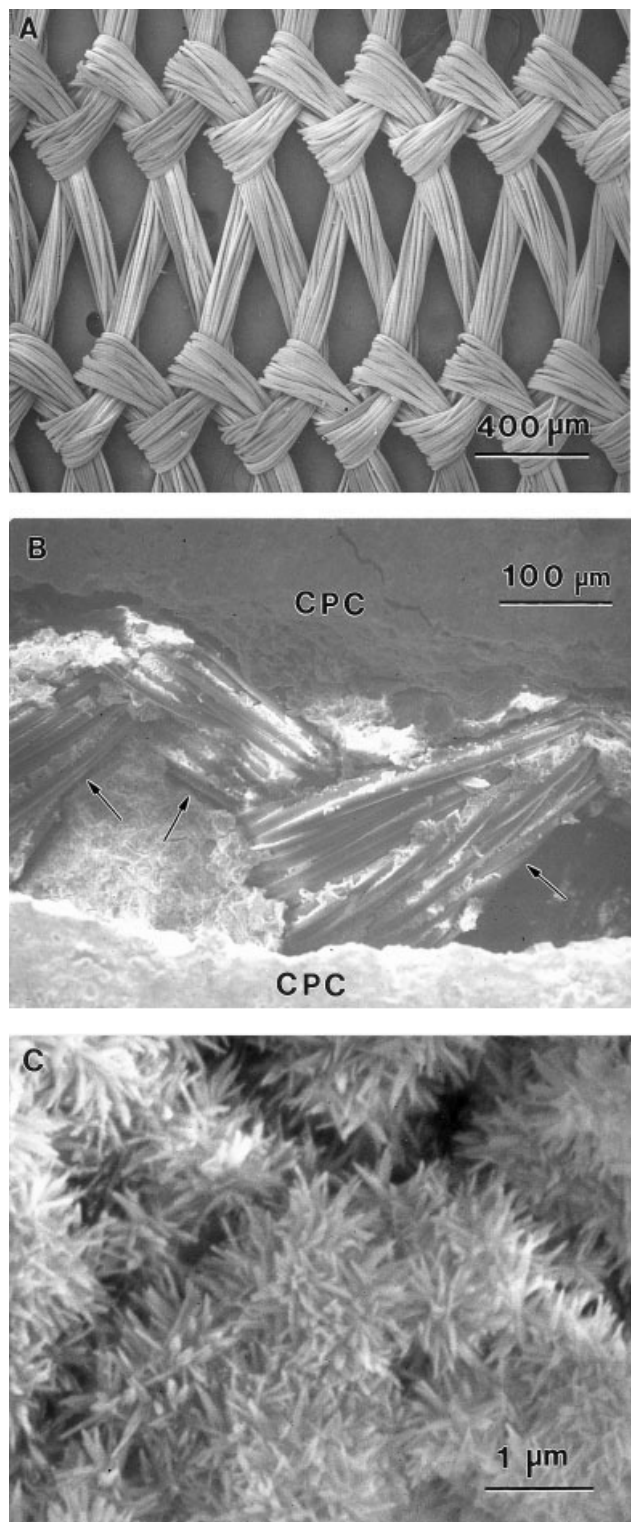
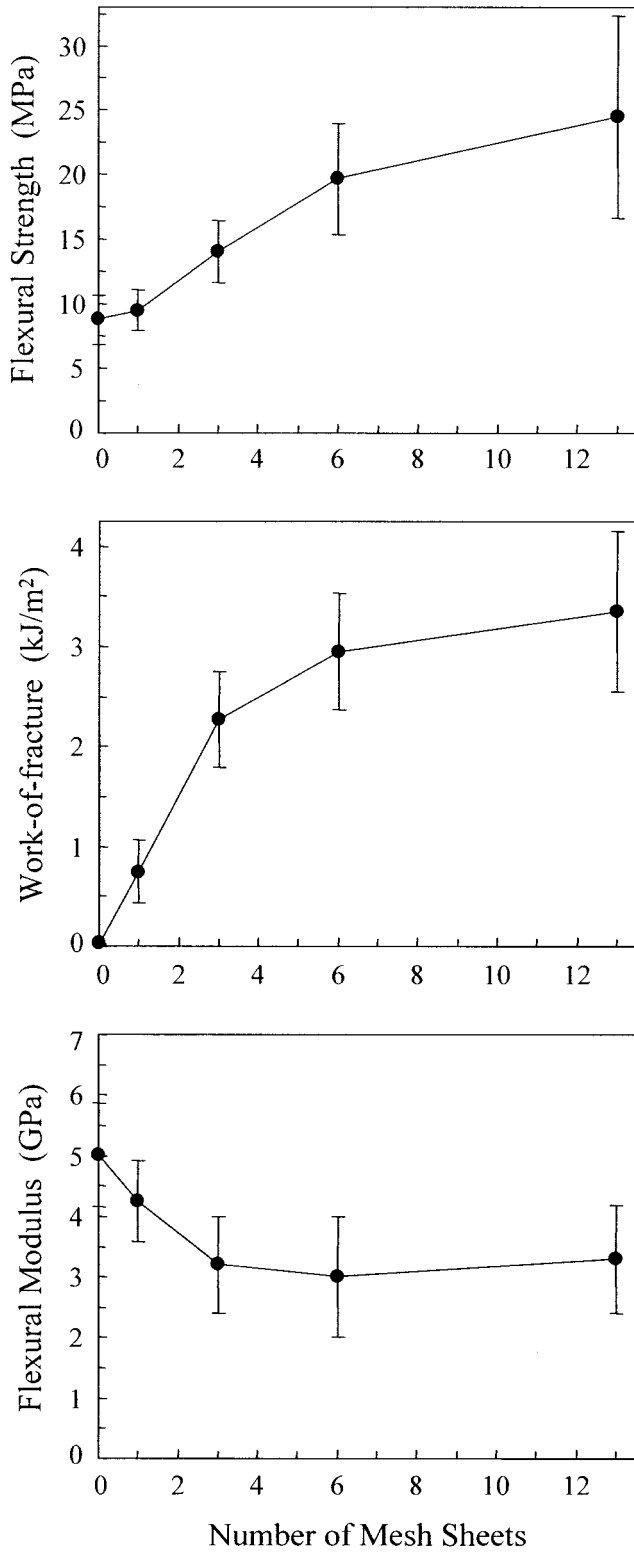


**Figure 1.** (A) SEM of an absorbable mesh. The fiber diameter is approximately  $14\ \mu\text{m}$ ; that of the bundle is  $140\ \mu\text{m}$ . The mesh thickness was approximately  $230\ \mu\text{m}$ . (B) SEM of mesh in CPC supporting the applied load in three-point flexure. Arrows in (B) indicate the mesh bridging the matrix crack and preventing the specimen from being separated by the applied stresses. (C) Hydroxyapatite crystals in CPC-mesh were similar to those in CPC control without mesh, indicating that the mesh incorporation did not retard the hydroxyapatite crystal formation.

failed catastrophically in a brittle manner. The mesh-reinforced specimens showed noncatastrophic fracture with the fiber mesh supporting the applied load in three-point flexure and keeping the multiple-cracked matrix intact [Figure 1(B)]. Figure 1(C) shows hydroxyapatite crystals in a CPC-mesh specimen. The crystals were approximately  $200\text{--}500\ \text{nm}$  in length and  $20\text{--}50\ \text{nm}$  in diameter. These elongated nano-crystals were observed to be similar in CPC-mesh composites and in CPC control without mesh, indicating that the incorporation of mesh did not retard the hydroxyapatite crystal formation.

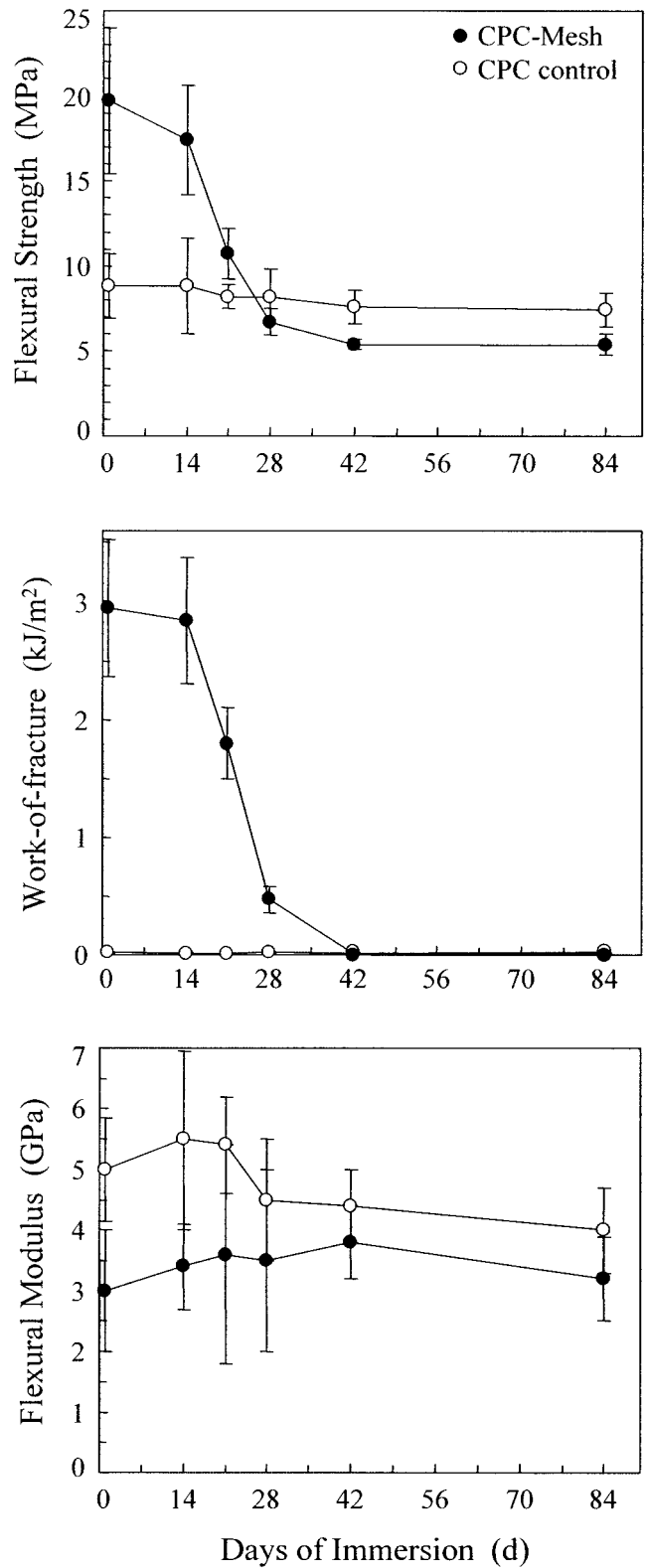
Effects of mesh number on mechanical properties are shown in Figure 2. The flexural strengths (mean  $\pm$  SD;  $n = 6$ ) of CPC containing 13 or 6 sheets of mesh were  $24.5 \pm 7.8$  and  $19.7 \pm 4.3$  MPa, respectively, not significantly different from each other (Tukey's multiple comparison; family confidence coefficient = 0.95). The strength of CPC with 13 meshes was significantly higher than, whereas that at 6 meshes was not significantly different from, the strength of  $14.0 \pm 2.0$  MPa for CPC containing 3 meshes. CPC with 6 or 13 meshes had higher strengths than that with 1 mesh; the strength of CPC with 3 meshes was not significantly different from  $9.5 \pm 1.6$  MPa of CPC with 1 mesh. The strengths of CPC containing 13 or 6 sheets of mesh were significantly higher than  $8.8 \pm 1.9$  MPa of CPC without mesh; the strengths at 3, 1, and 0 sheets of mesh were not significantly different from each other (Tukey's at family confidence coefficient of 0.95). The work-of-fracture of CPC with 6 or 13 meshes was  $2.95 \pm 0.58$  and  $3.35 \pm 0.80\ \text{kJ}/\text{m}^2$ , respectively; they are two orders of magnitude higher than  $0.021 \pm 0.006\ \text{kJ}/\text{m}^2$  of CPC without mesh. The elastic modulus of CPC without mesh was  $5.01 \pm 0.85$  GPa, significantly higher than  $3.02 \pm 0.99$  GPa with 6 sheets of mesh and  $3.28 \pm 0.89$  GPa with 13 sheets of mesh (Tukey's at family confidence coefficient of 0.95).

Effects of immersion time on mechanical properties are shown in Figure 3. For the CPC-mesh specimens (each with six sheets of mesh), the immersion time had significant effects on strength and work-of-fracture (analysis of variance;  $p < 0.001$ ), but not on modulus ( $p = 0.17$ ). For CPC without mesh, the immersion time did not have a significant effect ( $p = 0.55$  for strength,  $p = 0.37$  for work-of-fracture, and  $p = 0.06$  for modulus). At immersion days of 1 and 14, the strengths of the CPC-mesh specimens were nearly twice those of CPC without mesh. The strength then decreased as the meshes started to dissolve, becoming slightly lower than those of the CPC without mesh, because of the presence of macropores resulting from mesh dissolution. The work-of-fracture showed a similar trend, with the work-of-fracture value at 28 days of immersion being  $0.47 \pm 0.11\ \text{kJ}/\text{m}^2$ , significantly higher than  $0.018 \pm 0.009\ \text{kJ}/\text{m}^2$  of CPC without mesh ( $p < 0.01$ ). The modulus of the CPC-mesh and of the CPC control

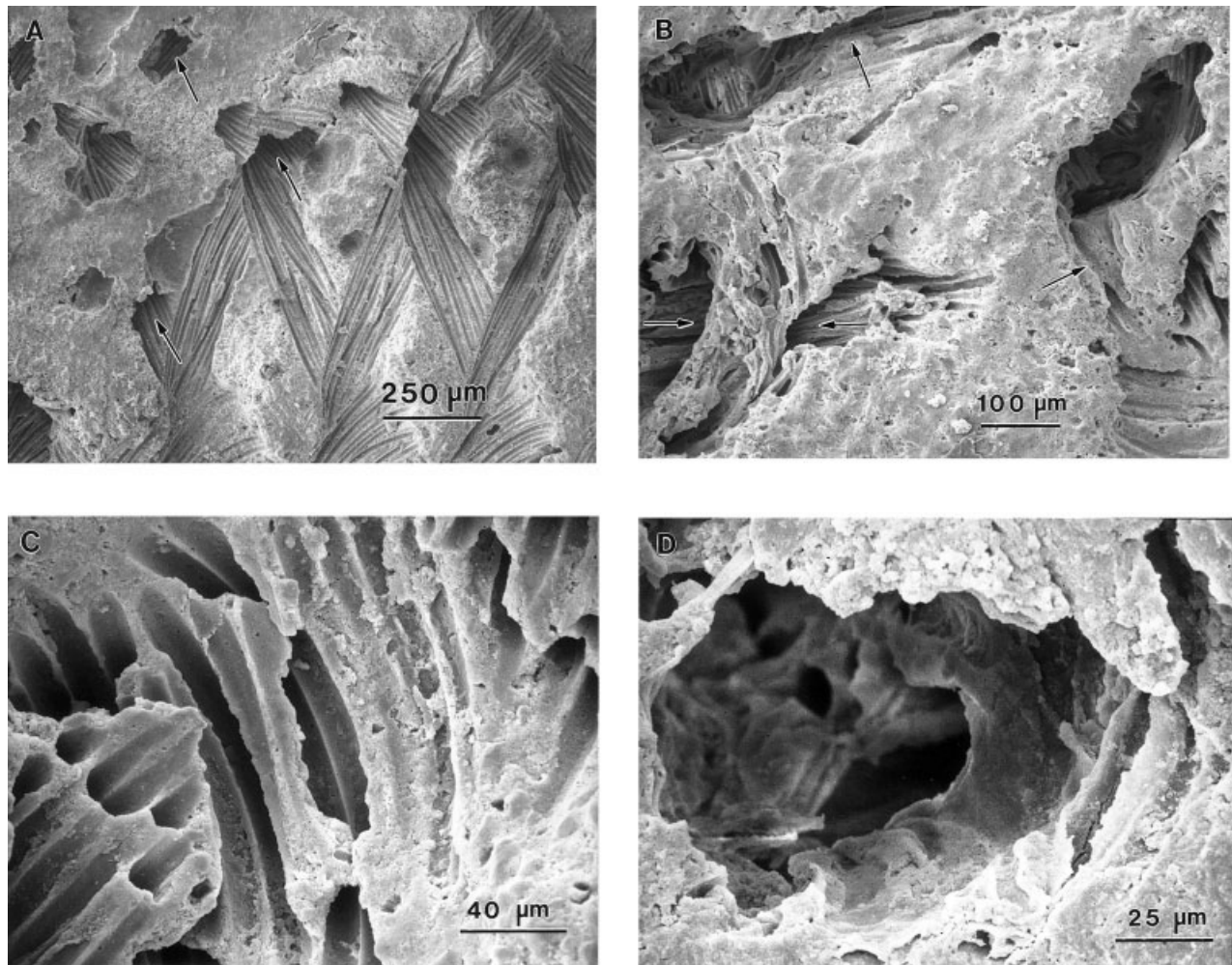


**Figure 2.** Flexural strength, work-of-fracture, and modulus versus the number of mesh sheets in the specimen. Each datum is the mean value of six measurements, with the error bar showing one standard deviation.

specimens were statistically similar at different immersion times (Tukey's at family confidence coefficient = 0.95).



**Figure 3.** Flexural strength, work-of-fracture, and modulus as a function of days of immersion. An intermediate number of six sheets of mesh was incorporated into the prospective tensile side of the CPC-mesh specimen. Each datum is the mean value of six measurements, with the error bar showing one standard deviation.



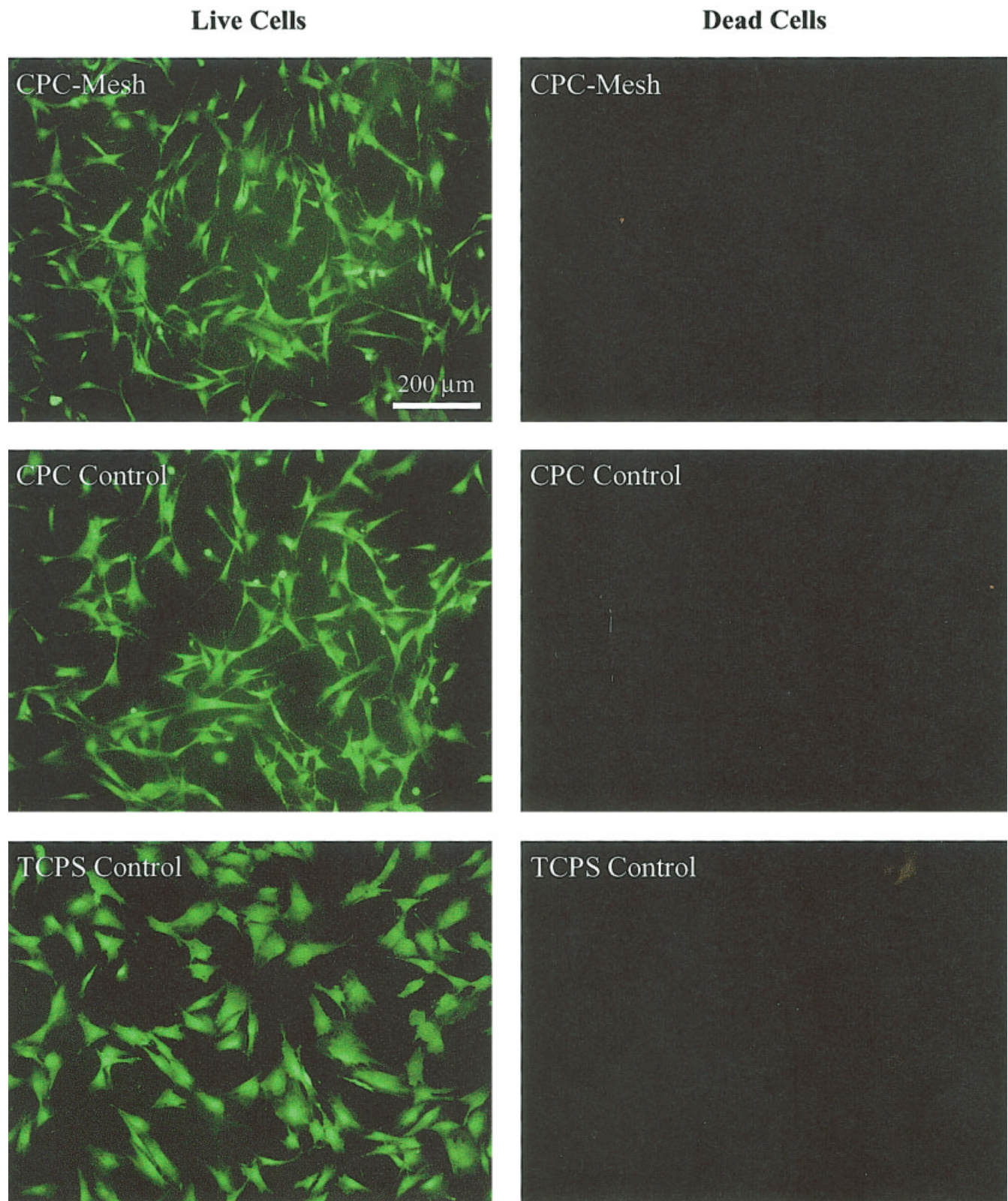
**Figure 4.** (A) SEM of CPC surfaces parallel to the mesh after mesh dissolution showing continuous macropore channels going into the CPC (arrows). The arrows in (B) indicate the interconnectivity of the pores. (C) Higher magnification of the wall of a macropore, which was full of small pores created by the dissolution of the individual fibers in the mesh bundle. (D) A typical macropore in the cross-section perpendicular to the stacked sheets of mesh.

Figure 4(A) shows macropores (arrows) going into CPC after mesh dissolution in 84 days' immersion. The pore structure resembled the appearance of the mesh. The arrows in Figure 4(B) indicate the interconnectivity of the pores. Figure 4(C) shows at a higher magnification the wall of a macropore, which was full of small pores created by the dissolution of the individual fibers of the mesh. The individual fibers in the mesh bundle were imprinted in the CPC matrix, because of intimate contact with the CPC paste during specimen fabrication. Some of the CPC-mesh specimens immersed for 84 days were cross-sectioned to reveal the interior plane perpendicular to the stacked sheets of mesh. Figure 4(D) shows a typical macropore in the cross-section.

Cells cultured for 1 day on CPC-mesh, CPC control, and TCPS control specimens were viewed with fluorescence microscopy and are shown in Figure 5. The live cells were stained green whereas the dead cells were stained red. The live cells appeared to have

adhered and attained a normal, polygonal morphology when seeded on all three materials. Visual examination revealed that the density of live cells adherent to each material appeared to be similar. All three materials had very few dead cells. An SEM micrograph of cells cultured for 1 day on CPC control is shown in Figure 6. The cells (large arrows) had polygonal shapes, with long processes (small arrows) attached to the surface of CPC. These features were observed to be similar to those on CPC-mesh and TCPS control. Therefore, after 1 day of culture, cell adhesion and viability on CPC-mesh was the same as that on CPC control without mesh and on TCPS control.

Cells cultured for 14 days are shown in Figure 7. The live cells appeared to have formed a confluent monolayer by 14 days for both CPC-mesh, CPC control, and TCPS control. The live cell density on all three materials appeared similar, demonstrating that cells adhered and proliferated equally well on these



**Figure 5.** MC3T3-E1 cells were seeded onto CPC-mesh, CPC control, and TCPS control (tissue culture polystyrene wells), incubated for 1 day, and prepared for fluorescence microscopy. Cells were double-stained to be green for live cells and red for dead cells.

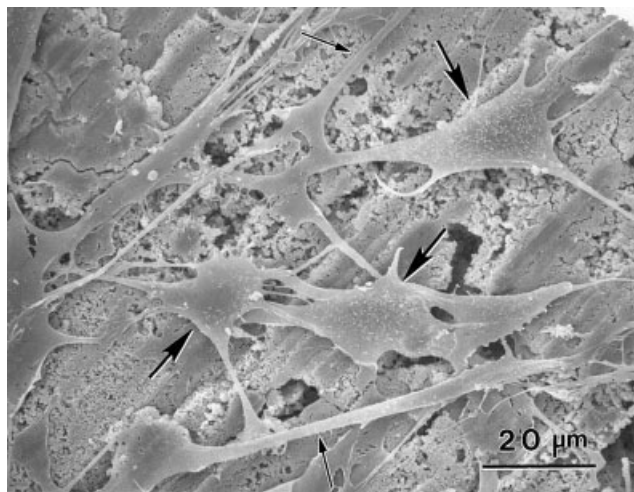


**Figure 6.** SEM of cells 1 day after being seeded onto a CPC control specimen. The cells attained a normal polygonal morphology (indicated by the large arrows) with long processes (small arrows) that were attached to the specimen surface. These characteristics were similar for CPC control, CPC-mesh, and TCPS control specimens.

three materials. The density of live cells in Figure 7 at 14 days was much greater than the density of live cells in Figure 5 (1 day), indicating that the cells had greatly proliferated between 1 and 14 days. Dead cells were very few on all three materials. These results suggest that cell proliferation and viability after 2 weeks of culture on CPC-mesh was the same as on CPC control without mesh and on TCPS control, demonstrating that the CPC-mesh composite was as biocompatible as CPC control and TCPS control.

The quantitative assessment of cell viability at 14 days using the Wst-1 assay is shown in Figure 8. The Wst-1 assay on cells cultured on TCPS was not performed because the growth area of the 24-well TCPS plates was not equivalent to the growth area on the cement discs and would not allow an accurate comparison. Horizontal line shows that a similar amount of dehydrogenase activity was present in cells cultured on CPC-mesh or CPC control (Student's *t* test;  $p > 0.1$ ). This is consistent with the live and dead cell examinations showing that the new CPC-mesh composite was as biocompatible as the CPC control without mesh.

## DISCUSSION

This study combined the superior reinforcement of mesh with the benefit of macropores in a self-hardening and resorbable hydroxyapatite composite for dental, craniofacial, and orthopedic repairs. Absorbable meshes were used to reinforce the hydroxyapatite cement to provide high strength and toughness, and then were dissolved to create interconnected macro-

pores suitable for bone ingrowth. As a result, the strength of CPC nearly tripled, and work-of-fracture (toughness) increased by two orders of magnitude. The dissolution of mesh created interconnected macropore channels in CPC with equivalent diameters of approximately 100–200  $\mu\text{m}$ . When implanted *in vivo*, the meshes should degrade to expose macropores for bony ingrowth. The strengthening of the graft from bony ingrowth and the deposition of new bone<sup>33–35</sup> should offset the weakening of the graft caused by mesh degradation. The mesh fibers appeared to be well wetted by the CPC matrix, manifested by the fiber mesh being firmly held by the CPC matrix during crack-bridging [Fig. 1(B)], and by the imprints of the individual fibers in the matrix after mesh dissolution [Fig. 4(A,C)]. The relatively rough surfaces of the mesh bundles and nodes probably enhanced the interlocking in the matrix. Previous studies observed matrix CPC pieces on the fiber surfaces after fiber pullout because hydroxyapatite was able to crystallize onto the fiber surfaces during CPC paste setting, suggesting a CPC-fiber interface as strong as the CPC itself.<sup>25</sup> The reinforcement mechanism appeared to be the fiber mesh bridging matrix cracks to resist their further opening and propagation, consistent with previous studies.<sup>29</sup> The matrix multiple cracks also consumed energy in creating new surfaces. In contrast, the CPC without mesh failed in a single crack. In addition, the frictional sliding and stretching of the mesh during pullout likely have contributed to the reinforcement efficacy.

The number of sheets of mesh incorporated in CPC significantly affected the composite strength and work-of-fracture (toughness). Three types of potential applications are mentioned here regarding the number of mesh sheets. First, in restoring thin bones, one sheet of mesh could be placed on the prospective tensile side of the CPC. One sheet of mesh, although not improving the strength, did increase the work-of-fracture (or toughness) by 35 times. Potential applications utilizing a single mesh include craniofacial repairs such as the reconstruction of defects in parietal skull or in other shell structures. Other applications may include the restoration of tooth cavities. Second, several sheets of mesh could be stacked in the side of CPC that may experience flexural or tensile stresses. The stacked sheets of mesh would not only provide the needed strength and toughness, but would also dissolve to create an external layer in CPC containing interconnected macropores to accept bone ingrowth. The growth of bone into this macroporous surface layer would provide a large interfacial area and enhance the implant fixation in its host. For example, when CPC alone was used in periodontal bone repair, tooth mobility resulted in early fracture and eventual exfoliation of the rigid and brittle implants.<sup>13</sup> Therefore, the CPC-mesh composite would be beneficial not

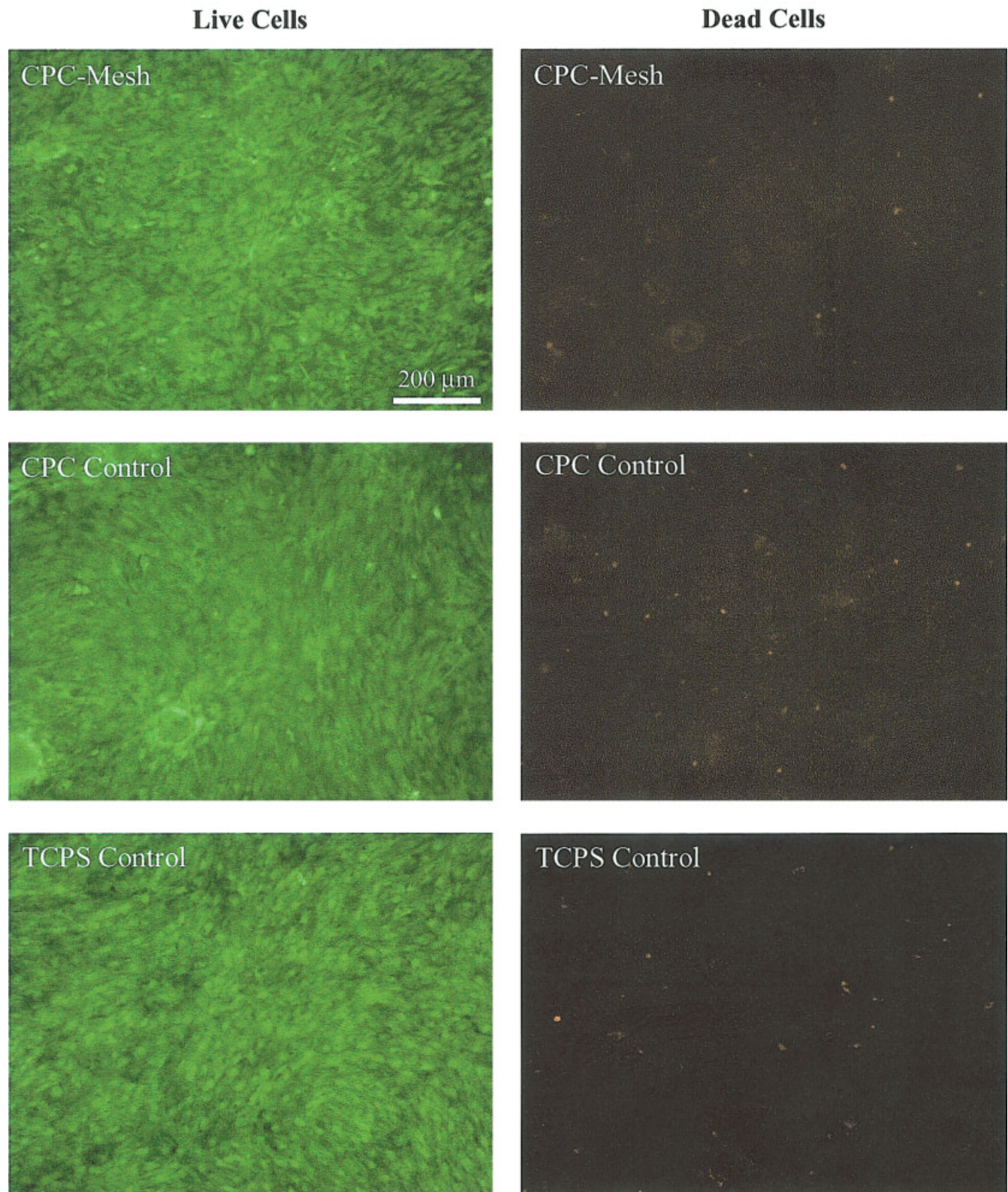


**Figure 7.** MC3T3-E1 cells were seeded onto CPC-mesh, CPC control, and TCPS control, incubated for 14 days and prepared for fluorescence microscopy. Cells were double-stained to be green for live cells and red for dead cells.

only because of the substantial increases in strength and fracture resistance, but also the presence of macropores to facilitate integration of CPC with adja-

cent bone. Third, the sheets of mesh could be stacked throughout the entire cavity, with the CPC paste filling the mesh holes and setting into a solid hydroxy-

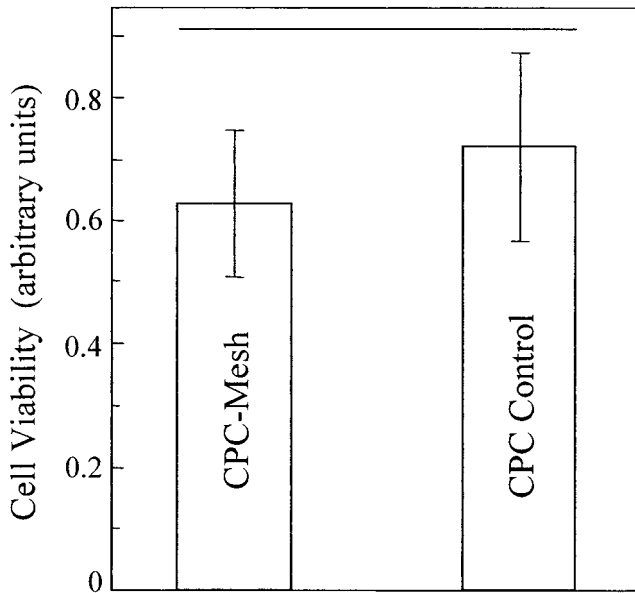


**Figure 8.** MC3T3-E1 cells were seeded onto CPC-mesh and CPC control, incubated for 14 days, and analyzed for viability with the Wst-1 assay. The Wst-1 assay is a colorimetric assay of cellular dehydrogenase activity and the absorbance at 450 nm is proportional to the amount of dehydrogenase activity in the cells on the discs. Error bars show standard deviation with  $n = 6$ . Horizontal line indicates statistically similar values (Student's  $t$  test;  $p > 0.1$ ).

apatite implant. This could achieve the maximum strength and toughness from the meshes, and then create interconnected macropores throughout the entire implant after mesh dissolution. For example, with 13 sheets of mesh in a specimen 3 mm thick, the short-term strength was increased by nearly three times and work-of-fracture by 150 times.

For random pore geometry, pore sizes of at least 100  $\mu\text{m}$  are required for bone ingrowth.<sup>36</sup> Previous studies have used hydroxyapatite implants with pores of an average diameter of 100 and 150  $\mu\text{m}$ .<sup>37,38</sup> Porous materials with random pore geometry generally have much smaller interconnecting fenestration than the pores themselves.<sup>22,37,39,40</sup> Therefore, the interconnection size is the limiting factor for osteoconduction, rather than the pores themselves. One study showed that pore interconnections  $<10$   $\mu\text{m}$  in diameter did not allow cell migration,<sup>37</sup> consistent with the SEM in Figure 6 of the present study showing mouse osteoblast cells of sizes 20–40  $\mu\text{m}$ . An *in vivo* study showed that a commercial porous hydroxyapatite, with pore size of 50–300  $\mu\text{m}$ , but much smaller pore interconnection diameters of 0.1–2  $\mu\text{m}$ , exhibited poor invasion of bone tissue into the implant. In contrast, a sintered hydroxyapatite with pore interconnection diameters of 2–100  $\mu\text{m}$  and an average of 40  $\mu\text{m}$ , which theoretically would permit cell migration or tissue invasion from pore to pore, exhibited superior new bone growth deep into the implant (3-mm penetration

in 6 weeks).<sup>37</sup> In the present study, to increase the pore interconnecting fenestration, absorbable meshes were used to reinforce CPC for the needed early strength and then to create highly interconnected macropores after mesh dissolution. The mesh bundles had diameters of 100–200  $\mu\text{m}$ , which after dissolution would create in CPC cylindrical macropores not only with a pore diameter of 100–200  $\mu\text{m}$ , but also with a pore interconnecting fenestration of the same size. Because the mesh fiber bundles [Fig. 1(A)] were completely interconnected and the mesh sheets were stacked on top of each other, the macropores formed in CPC after mesh dissolution should be highly interconnected and suitable for cell infiltration deep into the scaffold. Further study is needed to investigate the migration of osteoblast cells into the scaffold and the secretion of extracellular matrix components inside the scaffold, as a function of pore density and pore geometry. The interconnected macropore channels from the dissolution of mesh sheets are expected to not only improve bony ingrowth into the implant,<sup>20–23</sup> but also increase the rate of CPC dissolution, resorption, and replacement by new bone.<sup>24,25</sup>

Both CPC-mesh composite and CPC control were shown in the cell culture studies to be biocompatible. After 1 day of cell culture, osteoblast-like cells (MC3T3-E1) were able to adhere, spread, and remain viable on CPC-mesh, CPC control, and TCPS control when observed by fluorescence microscopy. At 14 days' cell cultures, fluorescence microscopy and the quantitative Wst-1 assay showed that cell adhesion, proliferation, and viability were equivalent on these materials. Therefore, these *in vitro* cell culture results suggest that the new CPC-mesh composite is biocompatible.

## CONCLUSION

The present study used a novel method that imparted substantial reinforcement and interconnected macropores to a moldable, self-hardening, and resorbable hydroxyapatite cement. Absorbable meshes were incorporated into CPC which resulted in substantially higher strength and toughness, with the formation of interconnected macropore channels after mesh dissolution. The nearly three times increase in strength and 150 times increase in work-of-fracture (toughness) for CPC may help extend its dental and orthopedic applications to the repair of moderate stress-bearing locations. The CPC paste-mesh could be shaped to fit various types of bone defects. When implanted *in vivo*, the meshes would degrade to form macropores for bony ingrowth. The strengthening of the CPC from new bone ingrowth would offset the weakening of CPC caused by mesh dissolution. The new CPC-mesh

formulation was shown to be biocompatible and supported the adhesion, spreading, proliferation, and viability of osteoblast-like cells *in vitro*. The novel method of combining superior strength and toughness of mesh reinforcement with interconnected and long cylindrical macropores for bone ingrowth may have wide applicability to other biomaterials.

The authors are grateful to Dr. J. B. Quinn and A. A. Giuseppetti for experimental assistance, and Drs. F. C. Eichmiller, G. E. Schumacher, S. Takagi, L. C. Chow, and J. R. Kelly for discussions.

## References

- Hench LL. Bioceramics. *J Am Ceram Soc* 1998;81:1705-1728.
- Suchanek W, Yoshimura M. Processing and properties of hydroxyapatite-based biomaterials for use as hard tissue replacement implants. *J Mater Res* 1998;13:94-117.
- Brown WE, Chow LC. A new calcium phosphate water setting cement. In: Brown PW, editor. *Cements research progress*. Westerville, OH: American Ceramic Society; 1986. p 352-379.
- Ginebra MP, Fernandez E, De Maeyer EAP, Verbeeck RMH, Boltong MG, Ginebra J, Driessens FCM, Planell JA. Setting reaction and hardening of an apatite calcium phosphate cement. *J Dent Res* 1997;76:905-912.
- Constantz BR, Barr BM, Ison IC, Fulmer MT, Baker J, McKinney L, Goodman SB, Gunasekaran S, Delaney DC, Ross J, Poser RD. Histological, chemical, and crystallographic analysis of four calcium phosphate cements in different rabbit osseous sites. *J Biomed Mater Res* 1998;43:451-461.
- Miyamoto Y, Ishikawa K, Takechi M, Toh T, Yuasa T, Nagayama M, Suzuki K. Histological and compositional evaluations of three types of calcium phosphate cements when implanted in subcutaneous tissue immediately after mixing. *J Biomed Mater Res* 1999;48:36-42.
- Friedman CD, Costantino PD, Jones K, Chow LC, Pelzer HJ, Sisson GA. Hydroxyapatite cement. II. Obliteration and reconstruction of the cat frontal sinus. *Arch Otolaryngol Head Neck Surg* 1991;117:385-389.
- Friedman CD, Costantino PD, Takagi S, Chow LC. Bone-Source™ hydroxyapatite cement: a novel biomaterial for craniofacial skeletal tissue engineering and reconstruction. *J Biomed Mater Res* 1998;43:428-432.
- Shindo ML, Costantino PD, Friedman CD, Chow LC. Facial skeletal augmentation using hydroxyapatite cement. *Arch Otolaryngol Head Neck Surg* 1993;119:185-190.
- Costantino PD, Friedman CD, Jones K, Chow LC, Sisson GA. Experimental hydroxyapatite cement cranioplasty. *Plast Reconstr Surg* 1992;90:174-191.
- Chohayeb AA, Chow LC, Tsaknis P. Evaluation of calcium phosphate as a root canal sealer-filler material. *J Endod* 1987;13:384-387.
- Sugawara A, Chow LC, Takagi S, Chohayeb H. *In vitro* evaluation of the sealing ability of a calcium phosphate cement when used as a root canal sealer-filler. *J Endod* 1990;16:162-165.
- Brown GD, Mealey BL, Nummikoski PV, Bifano SL, Waldrop TC. Hydroxyapatite cement implant for regeneration of periodontal osseous defects in humans. *J Periodontol* 1998;69:146-157.
- Pourdeyhimi B, Wagner HD. Elastic and ultimate properties of acrylic bone cement reinforced with ultra-high-molecular-weight polyethylene fibers. *J Biomed Mater Res* 1989;23:63-80.
- Goldberg AJ, Burstone CJ, Hadjinkolaou I, Jancar J. Screening of matrices and fibers for reinforced thermoplastics intended for dental applications. *J Biomed Mater Res* 1994;28:167-173.
- Topoleski LDT, Ducheyne P, Cuckler JM. The effects of centrifugation and titanium fiber reinforcement on fatigue failure mechanisms in poly(methyl methacrylate) bone cement. *J Biomed Mater Res* 1995;29:299-307.
- von Gonten AS, Kelly JR, Antonucci JM. Load-bearing behavior of a simulated craniofacial structure fabricated from a hydroxyapatite cement and bioresorbable fiber-mesh. *J Mater Sci Mater Med* 2000;11:95-100.
- Xu HHK, Eichmiller FC, Giuseppetti AA. Reinforcement of a self-setting calcium phosphate cement with different fibers. *J Biomed Mater Res* 2000;52:107-114.
- Xu HHK, Eichmiller FC, Barndt PR. Effects of fiber length and volume fraction on the reinforcement of calcium phosphate cement. *J Mater Sci Mater Med* 2001;12:57-65.
- Holmes RE, Bucholz RW, Monney V. Porous hydroxyapatite as a bone-graft substitute in metaphyseal defects. *J Bone Joint Surg* 1986;68:904-911.
- Eggl PS, Muller W, Schenk RK. Porous hydroxyapatite and tricalcium phosphate cylinders with two different pore size ranges implanted in the cancellous bone of rabbits. *Clin Orthop* 1988;232:127-138.
- Magan A, Ripamonti U. Geometry of porous hydroxyapatite implants influences osteogenesis in baboons (*Papio ursinus*). *J Craniofac Surg* 1996;7:71-78.
- Chang BS, Lee CK, Hong KS, Youn HJ, Ryu HS, Chung SS, Park KW. Osteoconduction at porous hydroxyapatite with various pore configurations. *Biomaterials* 2000;21:1291-1298.
- Takagi S, Chow LC. Formation of macropores in calcium phosphate cement implants. *J Mater Sci Mater Med* 2001;12:135-139.
- Xu HHK, Quinn JB, Takagi S, Chow LC, Eichmiller FC. Strong and macroporous calcium phosphate cement: effects of porosity and fiber reinforcement on mechanical properties. *J Biomed Mater Res* 2001;57:457-466.
- Xu HHK, Quinn JB. Calcium phosphate cement containing resorbable fibers for short-term reinforcement and macroporosity. *Biomaterials* 2002;23:193-202.
- ISO 10993-5. Biological evaluation of medical devices. Part 5. Tests for *in vitro* cytotoxicity. Geneva, Switzerland: International Standards Organization; 1999.
- American Society for Testing and Materials. ASTM F417-78: standard test method for flexural strength of electrical grade ceramics. Philadelphia, PA: American Society for Testing and Materials; 1984.
- Xu HHK, Ostertag CP, Braun LM, Lloyd IK. Short-crack mechanical properties and failure mechanisms of Si<sub>3</sub>N<sub>4</sub>-matrix/SiC-fiber composites. *J Am Ceram Soc* 1994;77:1889-1896.
- Simon CG Jr, Khatri CA, Wight SA, Wang FW. Preliminary report on the biocompatibility of a moldable, resorbable, composite bone graft consisting of calcium phosphate cement and poly(lactide-co-glycolide) microspheres. *J Orthop Res* 2002;20:473-482.
- Attawia MA, Uhrich KE, Botchwey E, Langer R, Laurencin CT. *In vitro* bone biocompatibility of poly(anhydride-co-imides) containing pyromellitylimidoalanine. *J Orthop Res* 1996;14:445-454.
- Ishiyama M, Shiga M, Sasamoto K, Mizoguchi M, He P-G. A new sulfonated tetrazolium salt that produces a highly water-soluble formazan dye. *Chem Pharm Bull* 1993;41:1118-1122.
- Holmes R, Mooney V, Bucholz R, Tencer A. A coralline hydroxyapatite bone graft substitute. *Clin Orthop* 1984;188:252-262.
- Piecuch JF, Goldberg AJ, Shastry CV. Compressive strength of implanted porous replamineform hydroxyapatite. *J Biomed Mater Res* 1984;18:39-45.

35. Martin RB, Chapman MW, Holmes RE, Sartoris DJ, Shors EC, Gordon JE, Heitter DO, Sharkey NA, Zissimos AG. Effects of bone ingrowth on the strength and non-invasive assessment of a coralline hydroxyapatite material. *Biomaterials* 1989;10:481-488.
36. Simske SJ, Ayers RA, Bateman TA. Porous materials for bone engineering. *Mater Sci Forum* 1997;250:151-182.
37. Tamai N, Myoui A, Tomita T, Nakase T, Tanaka J, Ochi T, Yoshikawa H. Novel hydroxyapatite ceramics with an interconnective porous structure exhibit superior osteoconduction *in vivo*. *J Biomed Mater Res* 2002;59:110-117.
38. Pilliar RM, Filiaggi MJ, Wells JD, Grynblas MD, Kandel RA. Porous calcium polyphosphate scaffolds for bone substitute applications: *in vitro* characterization. *Biomaterials* 2001;22:963-972.
39. Hulbert SF, Morrison SJ, Klawitter JJ. Tissue reaction to three ceramics of porous and non-porous structures. *J Biomed Mater Res* 1972;6:347-374.
40. Holmes RE, Bucholz RW, Monney V. Porous hydroxyapatite as a bone-graft substitute in metaphyseal defects. *J Bone Joint Surg* 1986;68:904-911.